

Review

# A Review of the Mineralogy, Petrography, and Geochemistry of Serpentinite from Calabria Regions (Southern Italy): Problem or Georesource?

Rosalda Punturo <sup>1,2</sup>, Roberto Visalli <sup>1,\*</sup>  and Rosolino Cirrincione <sup>1</sup>

<sup>1</sup> Department of Biological, Geological and Environmental Sciences, University of Catania, 95129 Catania, Italy; punturo@unict.it (R.P.); rosolino.cirrincione@unict.it (R.C.)

<sup>2</sup> Institute of Environmental Geology and Geoengineering (IGAG), National Research Council (CNR), 00185 Rome, Italy

\* Correspondence: rvisalli@unict.it

**Abstract:** Serpentinite rocks testify to the ocean-floor metamorphism that took place and transformed the original mineralogy and fabric of previous ultramafic rocks. Due to their tectonic and petrological importance, in recent decades, there has been increasing interest in serpentinites. From the economic point of view, it is worth noting that, due to their beauty and attractiveness, serpentinite rocks have been exploited and traded as building and ornamental stones since prehistorical times worldwide. In this work, we provide a comprehensive report of the petrographic, mineralogical, petrophysical, and geochemical features of the serpentinites cropping out in the northern sector of the Calabria–Peloritani Orogen (Italy), where the historical quarries are located. Since these serpentinite rocks have been traded for a long time and employed as an excellent building material, their detailed knowledge may provide a useful tool to understand their behavior when they are employed as building materials, to predict their performances upon emplacement in monuments, and to plan correct restoration by considering the provenance of the lithotypes employed. Moreover, comprehensive characterization is also particularly important because it has been reported that serpentinites from Calabria may contain asbestiform and other fibrous minerals, as testified by the occurrence of chrysotile, tremolite, and actinolite asbestos located within the veins, which could lead to health problems due to asbestos fiber exposure. Finally, serpentinite may be considered as an important potential CO<sub>2</sub> sequestration sink.

**Keywords:** greenstones; serpentinite; stone materials; asbestos



**Citation:** Punturo, R.; Visalli, R.; Cirrincione, R. A Review of the Mineralogy, Petrography, and Geochemistry of Serpentinite from Calabria Regions (Southern Italy): Problem or Georesource? *Minerals* **2023**, *13*, 1132. <https://doi.org/10.3390/min13091132>

Academic Editor: Jordi Ibanez-Insa

Received: 29 July 2023

Revised: 17 August 2023

Accepted: 24 August 2023

Published: 26 August 2023



**Copyright:** © 2023 by the authors. Licensee MDPI, Basel, Switzerland. This article is an open access article distributed under the terms and conditions of the Creative Commons Attribution (CC BY) license (<https://creativecommons.org/licenses/by/4.0/>).

## 1. Introduction

Serpentinite rocks testify to the ocean-floor metamorphism that took place and transformed the original mineralogy and fabric of previous ultramafic rocks [1,2]. Serpentinite rocks contain serpentine-group polymorphs such as chrysotile, lizardite, and antigorite, whose chemical formula is  $Mg_3Si_2O_5(OH)_4$ , as the main constituents and chlorite, brucite, magnetite, talc, amphiboles, and/or carbonates, together with remnants of the protolith, such as pyroxene and olivine, as accessory mineral phases. The association of serpentinite with mafic igneous rocks (i.e., metabasite rocks) and chert has long been referred to as ophiolites or the Steinmann Trinity [3,4].

Due to their tectonic and petrological importance, in recent decades, there has been an increasing interest in serpentinites. From the economic point of view, it is worth noting that, due to their beauty and attractiveness, serpentinite rocks have been exploited and traded as building and ornamental stones since prehistorical times worldwide.

Nevertheless, despite their importance as building materials, only a few studies focus on these lithotypes as ornamental stones, either for conservation–restoration or for new buildings (e.g., [5–11]).

In the southern Apennines (Calabria, southern Italy), the occurrences of extensive ophiolite outcrops, mainly made of serpentinite and metabasite rocks, allowed serpentinites to be marketed as greenstone and their wide use since prehistorical times [12–14].

From the petrological point of view, there is some literature dedicated to the Calabrian ophiolites, dealing with the tectonic, petrological, and geochemical features [15–26].

In this paper, we selected some key serpentinite outcrops where abandoned quarries are located. These sites are representative since they constitute a database for serpentinite from Calabria as an ornamental stone, which was exploited and traded until the very recent past and is widely used for external parts of religious and civil buildings, as well as for internal architectural elements (Figure 1).



**Figure 1.** Examples of Calabrian serpentinites adopted as ornamental stones for external parts of buildings (a,b) and for internal architecture (c,d).

Another important point to be addressed is that previous studies on serpentinite from the southern Apennines reported the presence of asbestos and asbestiform minerals, with particular regard to the quarries referred to as greenstone, where serpentinite was exploited in the past (e.g., [14,27,28]), which are potentially harmful to humans and pose health concerns.

This contribution focuses on serpentinites located in the northern sector of the Calabria–Peloritani Orogen (CPO [29]) from the Mt. Reventino, Conflenti, and Gimigliano quarries (Calabria region, Italy), attempting to understand their behavior when they are employed as building materials, in order to predict their performances upon emplacement in monuments. Moreover, since serpentinite from Calabria has been traded for a long time, detailed knowledge of it may provide a useful tool for studies concerning the provenance of serpentinite employed in monuments and to plan for correct restoration. For these reasons, we present a comprehensive report of the petrographic, mineralogical, and geochemical features of serpentinite from Calabria, cropping out in the Sila Piccola Massif (e.g., [29–31]), where the historical quarries are located. Moreover, we discuss their physical–mechanical properties such as the Uniaxial Compressive Strength (UCS), seismic behavior, and their relationship with rock fabric [32,33]; finally, we discuss aspects related to documented asbestos occurrences in serpentinite from Calabria since human activities like road construction, mining, and agriculture in ophiolite outcrops may potentially give rise to disturbances in serpentinite rocks and induce the release of asbestiform minerals in the surrounding environment, thus triggering mechanisms of hazardous exposure for the population [34–38].

## 2. Geology of Serpentinite Outcrops of Calabria Region

The CPO can be divided into two main sectors [29]: (a) the northern sector includes the Coastal Chain and Sila Massifs, where the oceanic units are enclosed between the pre-Mesozoic continental crustal rocks at the top and the Apennine carbonate units at the bottom [22,29–31]; (b) the southern sector comprises the Serre and Aspromonte Massifs in central-southern Calabria and the Peloritani Mountains in north-eastern Sicily, where only continental crust-derived units crop out [29,39–44].

In this work, we focused on the ophiolite rocks that are only exposed in the northern sector of the CPO. The latter can be described, from the bottom to the top, as a superposition of three main structural complexes [16], namely, (a) the lowermost Apennine Complex, constituted of a thick Mesozoic carbonate succession that is partly metamorphosed [45–48]; (b) the intermediate Liguride Complex composed of oceanic units, representing remnants of the Tethys ocean [20,49–52], originally involved in subduction and successively in the Europe-verging continent–continent collision events [53–55]; and (c) the uppermost Calabride complexes [29,56], made up of an almost continuous continental crust section generated during the late Variscan orogeny with its original Mesozoic sedimentary cover (the Longobucco Unit), which was exclusively affected by brittle deformation [57,58].

Overall, the entire ophiolite sequence comprises mantle-derived, serpentinitized, ultramafic rocks and ophicalcites cropping out in the area of Gimigliano–Mt. Reventino, (Figure 2) and the sedimentary cover consisting of either pelagic sediments, such as meta-radiolarite and Calpionella meta-limestone [59,60], or flyschoid-type sediments, shown by metapelite and metarenite rocks of uncertain age and interpreted as proximal terrigenous deposits [61]. On the basis of the geochemical signatures of the basaltic protoliths, a T-MORB affinity and a genesis from harzburgitic–lherzolitic rocks of the serpentinites are clearly recognized [12,48]. An HP/LT metamorphism ( $p = 0.9–1.1$  GPa;  $T = 350$  °C) is highlighted by the mineralogical assemblages of metabasite and metapelite rocks [22,49,62]. In particular, according to the literature, the entire ophiolitic sequence is affected by an antiform at Mount Reventino, where massive and banded lenses of metabasalts and serpentinites with irregular structures are deformed into tight folds, constituting the summit [22,23].

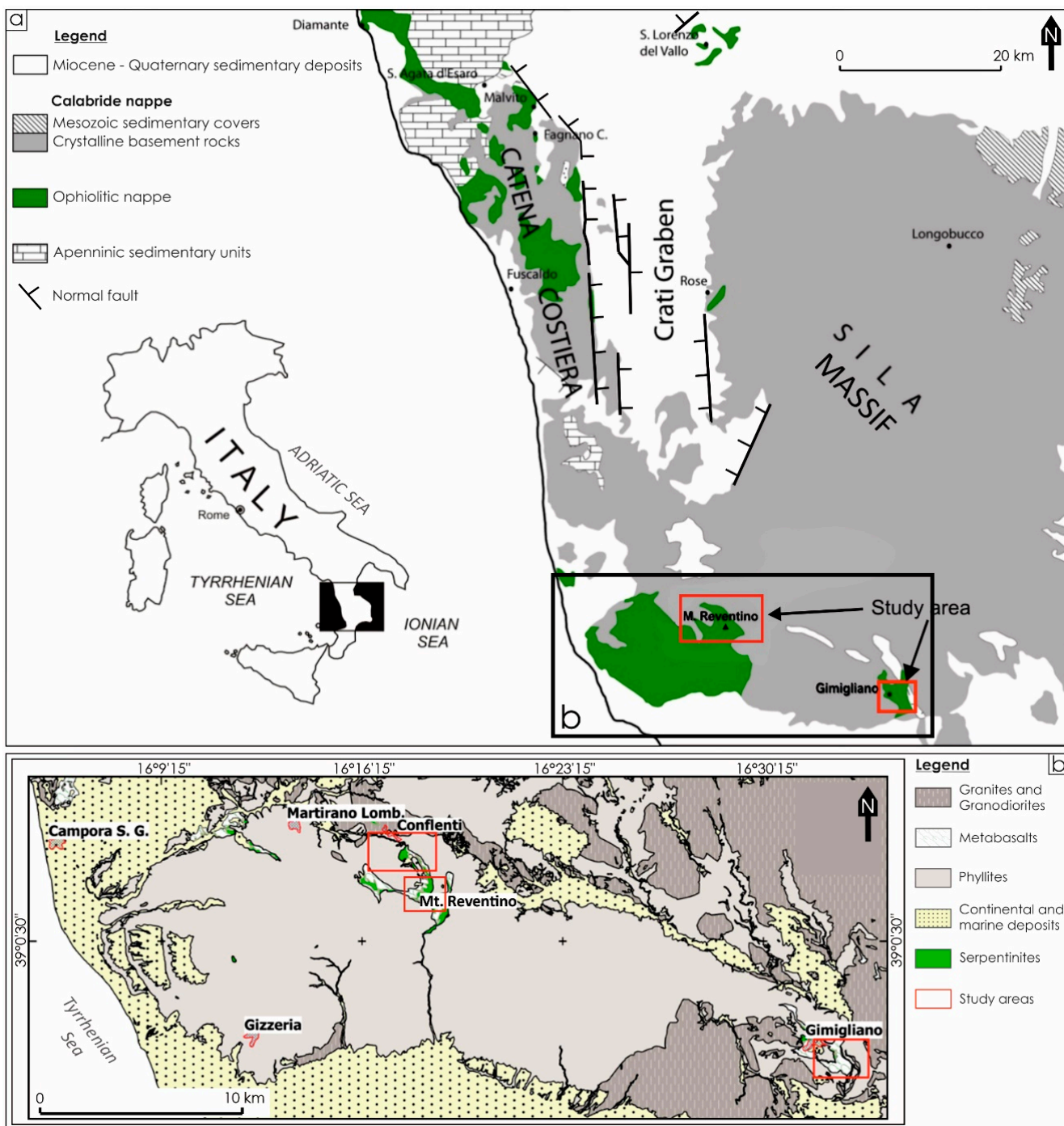


**Figure 2.** Geological sketch map of (a) the northern sector of the CPO with a focus on ophiolites' occurrence and study areas; (b) lithology of the study areas and the location of the sampling sites (modified after [14,63]).

Here, an abandoned quarry testifies to the exploitation of serpentinite as an ornamental stone until the very recent past (Figure 3). The other abandoned serpentinite quarries, which are considered to be representative of these lithotypes, are located near the San Mango and Gimigliano villages. In this paper, we present a summary of the results concerning these serpentinite sites on which the historical quarries sit.

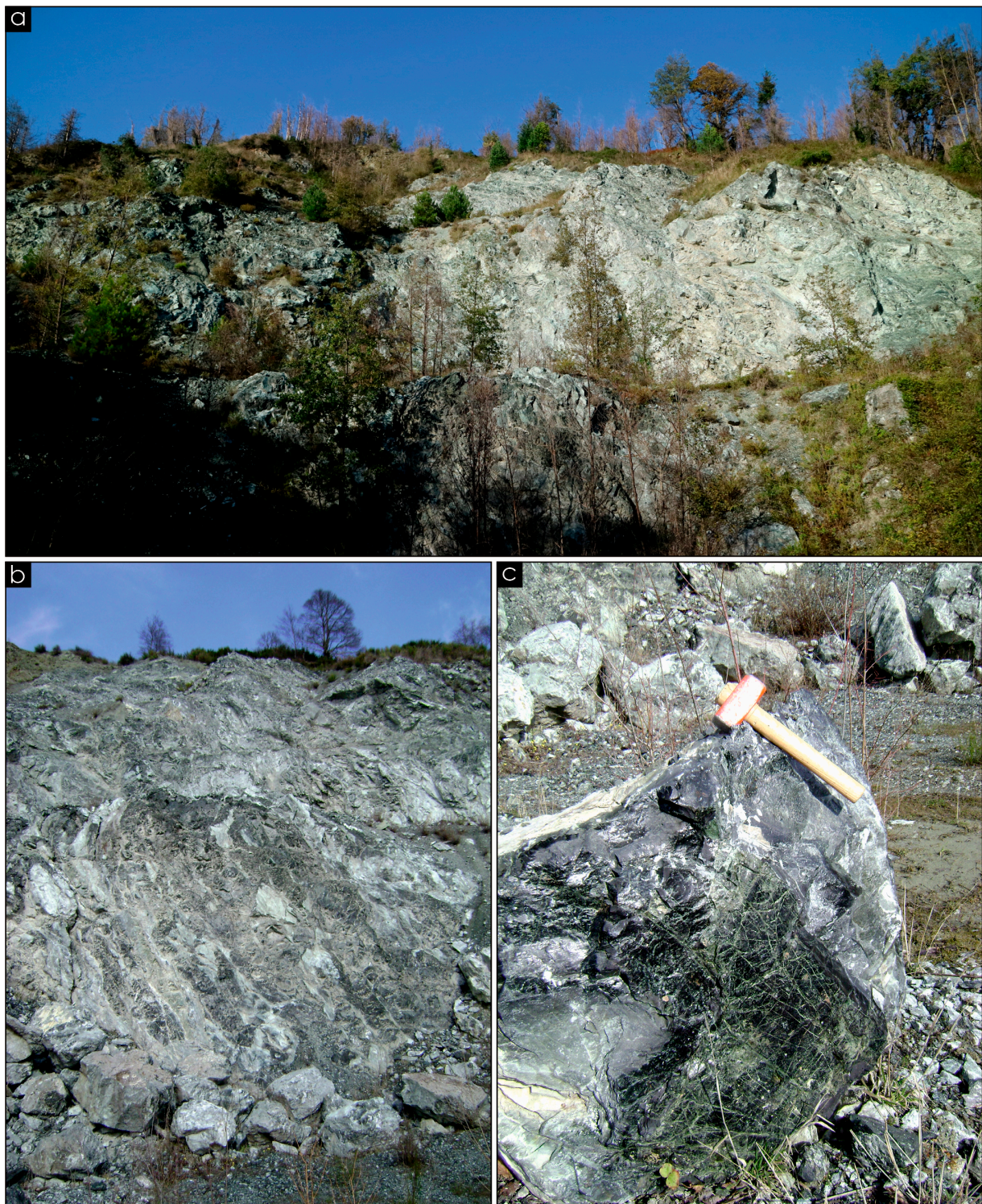


**Figure 3.** Abandoned quarries of serpentinite in Sila Piccola Massif, Calabria. (a) quarry located at Mt Reventino; (b) quarry located close to the village of Conflenti; (c) quarry located close to the village of Gimigliano.

### 3. Petrographic and Mineralogical Features

At the scale of the outcrop, serpentinites look massive and dark green in color (Figure 4a,b), with widespread network of fractures (Figure 4c). Along the road connecting the villages of San Mango and Conflenti, massive serpentinite is in alternation with weakly foliated portions of the same lithotype (Figure 4c). Moreover, some pieces exhibit a

blazing surface, which is typical of this lithotype, whereas, in some sites, several blocks of ophicalcite also occur, since calcite entirely surrounds the blocks of serpentine (Figure 4d). Various developed vein systems often crosscut the massive parts (Figure 4e,f).

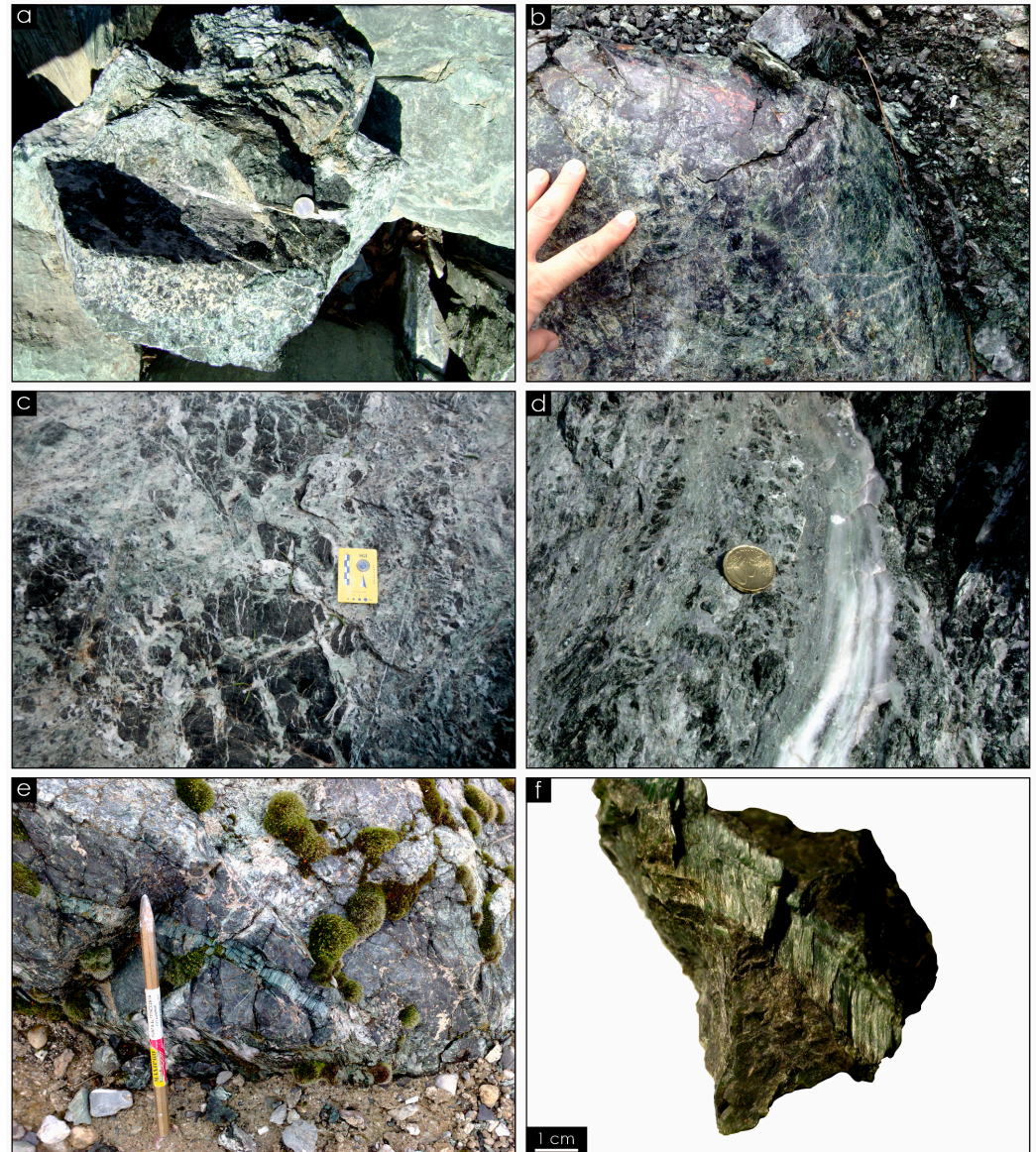


**Figure 4.** (a) Light- to (b) dark-green-colored serpentinite; (c) weak foliation and vein system; (d) ophicalcite at the mesoscale; (e) vein crosscutting the massive parts; and (f) detail of a vein in a selected specimen.

At the scale of the microscope, serpentinite exhibits a typical mesh microstructure (Figure 5a). Sometimes, it shows remnants of the original protogranular microstructure, which has been inherited from the ultramafic protolith (Figure 5a,b). The mineral assemblage is, on the whole, made of serpentine-group minerals (i.e., chrysotile, lizardite, and antigorite), magnetite  $\pm$  tremolite-actinolite  $\pm$  chlorite  $\pm$  clinopyroxene  $\pm$  Cr-spinel, and calcite (the latter of which is abundant in the ophicalcite samples). The serpentine-group minerals and small magnetite grains completely replaced the original olivine and orthopyroxene crystals and appear as pseudomorph aggregates with typical net-like and mesh microstructures (Figure 5c,d). Sometimes, orthopyroxene grains appear deeply replaced by green “bastite”; clinopyroxene occurs as millimetric grains or inclusions within the rare holly-leaf-shaped Cr-spinels of the original ultramafic rock (Figure 5c). It is worth noting

that, in most cases, original spinel grains are quite completely transformed into magnetite and chlorite. Different dilatation vein systems crosscut the massive bodies (Figure 4e,f); these veins are mainly composed of serpentine polymorphs and minor calcite together with talc flake aggregates and actinolite-tremolite fibers that may in part either fill the veins or occur within the serpentine matrix (Figure 5b). Serpentine fibers may be observed either as a breakage of the main matrix (Figure 6a,b) or they may be oriented either perpendicular to the vein selvages (“cross” serpentine) or according to their elongation directions (“lamellar” serpentine). Chrysotile fibers usually fill the veins in syntaxial growth showing a curvature of fibers in some veins (Figure 6c). The thickness of veins ranges from a few millimetres to (rare) 5–6 centimetres (Figures 4e,f and 5b) and are easily recognizable because of the bright color of serpentine, which varies from greyish green to bright green. Serpentine fibers are most cases arranged perpendicular to the vein elongation (Figure 6d). Scanning Electron Microscope (SEM) morphological observations [14,33] showed that most of the fibers, identified as chrysotile, are flexible. Lizardite with lamellar morphology occurs inside the massive serpentinite portions. Local longitudinal splitting of larger bundles into thinner (Figure 6a) or isolated fibrils. In the greyish green veins, sometimes whitish flakes have been observed. Small magnetite grains often mark the borders of the veins as well as are aligned along their central part (Figure 5b).

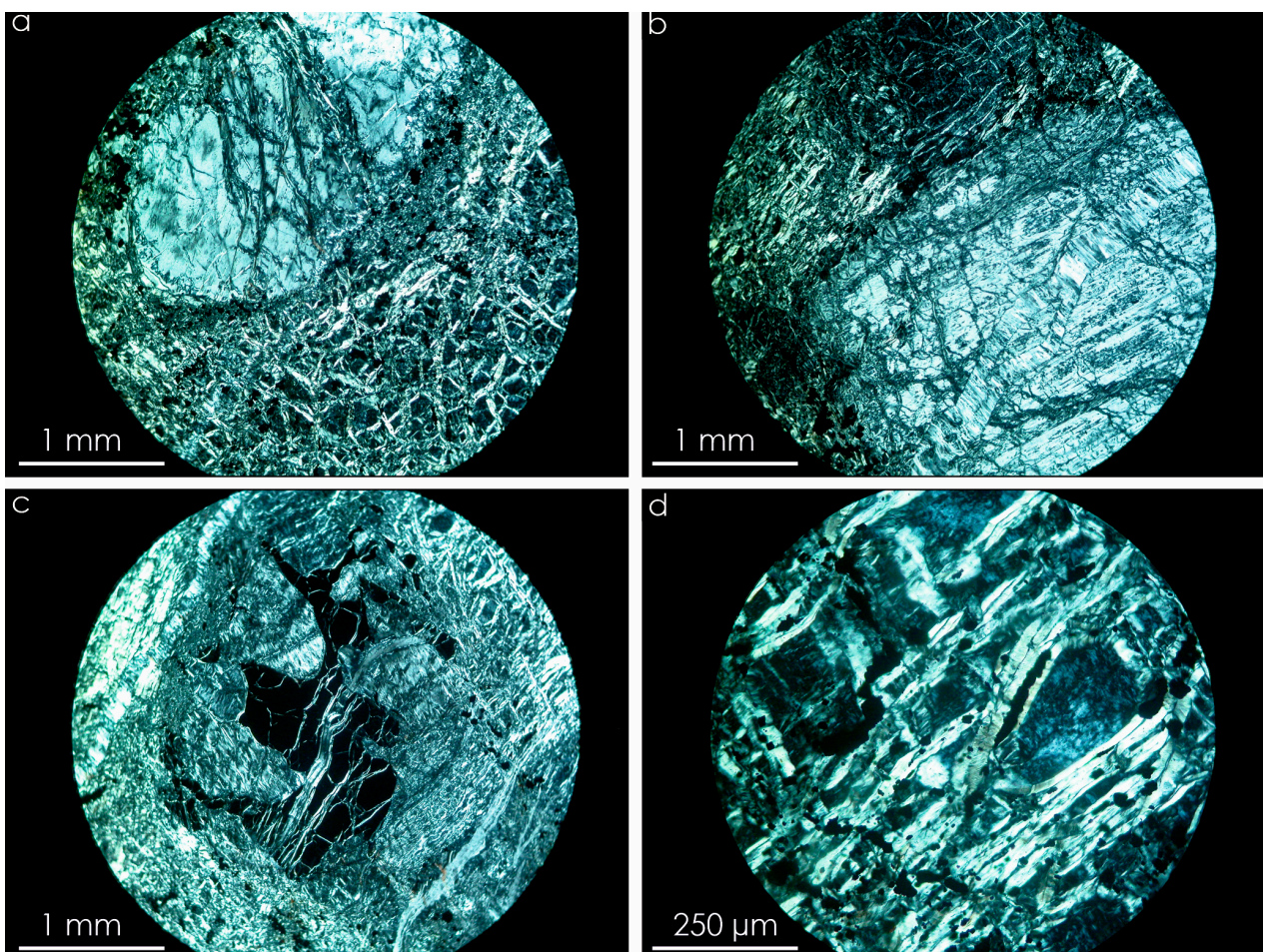


**Figure 5.** Photomicrograph of serpentinite from Calabria: (a) typical mesh microstructure and serpentine pseudomorph after primary mineral; (b) vein system development inside the matrix, with oriented magnetite; (c) magnetite pseudomorph after primary holly leaf spinel; (d) detail of mesh microstructure. Photomicrographs are taken under crossed polarizers conditions.

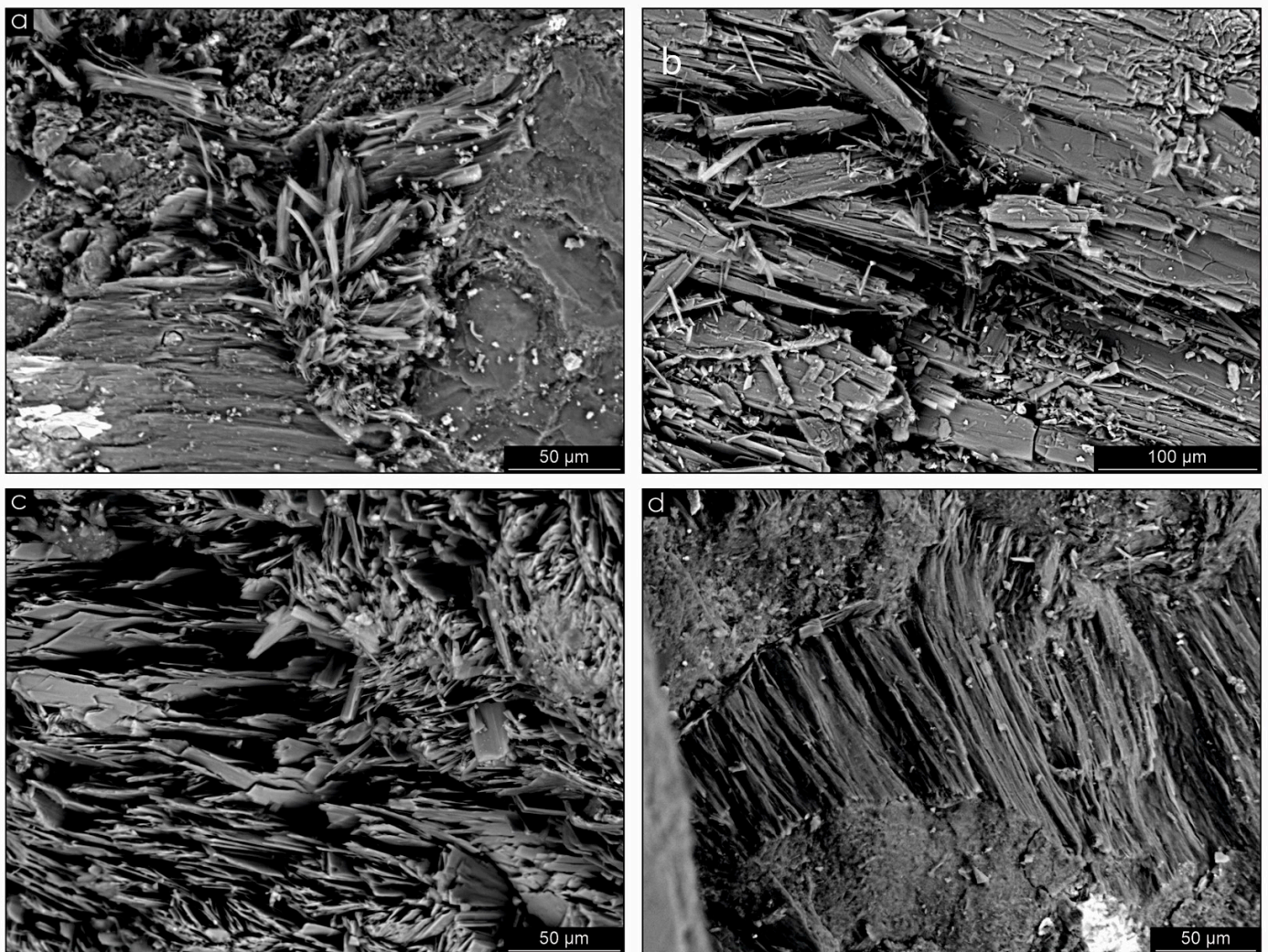


**Figure 6.** Scanning Electron Microscope pictures (modified after [14,33]). (a) fibrous serpentine flakes generating within the matrix; (b) lamellar serpentine polymorphs together with elongated crystals; (c) details of fibrous serpentine polymorphs and (d) elongation of fibrous serpentine within the vein.

#### 4. Geochemical Signatures of Serpentinites

In order to characterize, as a whole, the geochemical signatures of serpentinites from the investigated areas, representative bulk-rock data normalized to 100% from [12] and [48] (Tables 1–3) are compared and analyzed through the usage of both binary and discrimination diagrams. In the case of the binary diagrams,  $\text{Al}_2\text{O}_3$  was considered as the main variation index as Al is more appropriate to characterize the primary peridotite composition rather than secondary serpentinization [12]. The  $\text{Al}_2\text{O}_3$  content in the selected investigated samples shows the typical values of the oceanic peridotite [64].

**Table 1.** Major element oxides (wt%) concentrations of the representative serpentinites.

Sample	SiO <sub>2</sub>	TiO <sub>2</sub>	Al <sub>2</sub> O <sub>3</sub>	FeO <sub>tot</sub>	MnO	MgO	CaO	L.O.I.	Total	Mg#	Cr#
Gimigliano area											
gm1 *	45.9	0.0	4.0	8.2	0.1	42.1	0.1	12.6	100.3	79.9	13.7
gm2 *	45.9	0.0	1.6	8.5	0.1	44.1	0.1	11.9	100.3	80.0	22.8
gm3 *	45.8	0.0	2.9	9.3	0.1	42.0	0.1	12.9	100.3	77.7	13.5
gm4 *	46.2	0.0	1.7	8.0	0.1	44.3	0.0	11.7	100.3	81.1	23.9
gm6 *	44.9	0.0	2.6	8.1	0.1	43.1	1.6	13.8	100.3	80.5	14.0
gm7 *	43.4	0.0	1.5	8.4	0.1	43.0	3.7	14.1	100.3	79.8	17.9
gm9 *	46.2	0.0	2.9	8.5	0.1	42.3	0.2	12.9	100.3	79.3	14.6
gm10 *	45.9	0.0	1.8	8.5	0.1	42.9	1.1	13.3	100.3	79.7	22.2
DF3 *	44.7	0.1	2.0	7.7	0.1	44.0	1.3	14.0	100.0	81.6	23.1
Mt. Reventino area											
REV 1 *	46.3	0.0	1.6	7.8	0.1	44.6	0.0	12.0	100.4	81.7	19.7
REV 2 *	45.4	0.0	1.9	7.7	0.1	45.1	0.0	12.6	100.4	81.9	22.5
REV 3 *	44.8	0.0	2.7	7.9	0.1	44.5	0.3	12.3	100.3	81.4	19.9
REV 4 *	45.7	0.0	2.2	8.2	0.1	44.1	0.1	12.3	100.4	80.8	18.8
REV 6 *	44.5	0.1	3.1	9.7	0.1	42.5	0.4	13.1	100.3	77.3	19.8

\* Data from [12]; L.O.I. = Loss On Ignition; Mg# = magnesium number; Cr# = chromium number.

**Table 2.** Trace element (mg/kg) concentrations of the representative serpentinites from Gimigliano quarry.

Sample	gm1 *	gm2 *	gm3 *	gm4 *	gm6 *	gm7 *	gm9 *	gm10 *	DF3 *
Y	21.8	19.2	21.8	23.6	24.9	19.5	14.3	27.9	8.5
Nb	0.3	0.4	0.3	0.4	0.7	0.3	0.2	0.7	0.1
La	36.6	31.0	31.6	33.7	40.8	38.1	23.0	38.0	6.1
Ce	29.6	24.8	26.9	26.2	34.0	30.4	18.1	32.3	10.3
Pr	0.0	0.1	0.1	0.1	0.1	b.d.l.	0.0	0.2	0.1
Nd	0.1	0.3	0.2	0.2	0.4	0.1	0.1	0.5	0.3
Sm	0.0	0.0	0.1	0.0	0.1	0.0	0.0	0.1	0.1
Eu	0.0	0.0	0.1	0.1	0.1	0.1	0.0	0.1	0.0
Gd	0.3	0.2	0.3	0.3	0.3	0.2	0.2	0.4	0.2
Tb	0.0	0.0	0.1	0.0	0.1	0.0	0.1	0.1	0.0
Dy	0.4	0.2	0.4	0.2	0.4	0.2	0.4	0.5	0.3
Ho	0.1	0.1	0.1	0.1	0.1	0.1	0.1	0.2	0.1
Er	0.3	0.2	0.3	0.2	0.3	0.2	0.3	0.5	0.2
Tm	0.1	0.0	0.1	0.0	0.1	0.0	0.0	0.1	0.0
Yb	0.5	0.3	0.4	0.3	0.5	0.3	0.4	0.8	0.3
Lu	0.1	0.1	0.1	0.1	0.1	0.0	0.1	0.1	0.1
Cr	2905	2157	2070	2484	1938	1525	2297	2393	2772
Ni	1235	2051	1548	1938	1218	1825	1553	1829	1820
Rb	9.0	9.3	8.1	9.7	9.0	8.9	5.2	0.9	b.d.l.
Ba	b.d.l.	17.0							
Hf	2.3	3.0	2.4	3.2	2.9	2.4	1.6	7.5	0.0
Ta	0.1	0.1	0.0	0.1	0.1	0.0	0.1	0.1	0.0
Th	0.3	0.5	0.5	0.8	0.5	0.3	0.2	0.9	0.1
U	0.3	0.3	0.3	0.3	0.3	0.2	0.2	0.7	0.2
Sc	17.4	11.8	13.3	12.8	10.8	6.5	13.9	10.2	14.1
V	76.2	45.1	56.9	51.6	60.3	27.7	64.1	43.6	77.7
Co	79.3	104.3	100.2	99.3	80.1	97.2	99.0	107.5	110.7
Sr	b.d.l.	b.d.l.	b.d.l.	b.d.l.	b.d.l.	20.7	b.d.l.	b.d.l.	7.0
Zr	107.9	122.8	109.3	123.8	120.2	114.3	73.2	352.4	20.5
Zn	56.2	34.2	52.5	40.0	47.8	38.1	52.8	49.4	73.0

\* Data from [12]; b.d.l.: below detection limit.

**Table 3.** Trace element (mg/kg) concentrations of the representative serpentinites from the Mt. Reventino quarry.

Sample	REV 1 *	REV 2 *	REV 3 *	REV 4 *	REV 6 *
Y	8.0	10.3	8.8	14.6	14.1
Nb	0.8	0.3	0.1	1.0	0.3
La	7.1	7.2	6.6	12.0	11.9
Ce	12.3	18.5	11.6	20.4	18.6
Pr	0.8	0.1	0.1	0.2	0.6
Nd	2.8	0.5	0.5	1.0	2.1
Sm	0.3	0.1	0.1	0.2	0.3
Eu	0.06	0.1	0.04	0.1	0.1
Gd	0.30	0.4	0.21	0.4	0.4
Tb	0.04	0.0	0.04	0.1	0.1
Dy	0.16	0.3	0.23	0.4	0.6
Ho	0.04	0.1	0.06	0.1	0.1
Er	0.10	0.2	0.19	0.3	0.4
Tm	0.02	0.0	0.04	0.1	0.1
Yb	0.10	0.2	0.19	0.3	0.5
Lu	0.02	0.0	0.04	0.1	0.1
Cr	1773	2607	3100	2372	3524
Ni	1934	1937	1829	2133	2241
Rb	0.6	4.6	1.8	7.4	1.3
Ba	b.d.l.	b.d.l.	b.d.l.	b.d.l.	b.d.l.
Hf	0	1.9	0.5	5.8	0.4
Ta	1.6	0.0	0.0	0.6	0.0
Th	0.10	0.1	0.1	0.3	0.1
U	0.02	0.2	0.02	0.2	0.1
Sc	7.45	5.8	12.7	8.7	18.0
V	30	49.8	45	40	68
Co	105.0	87.4	103.4	105.7	129.7
Sr	3.1	13.1	9.1	5.5	8.6
Zr	9.0	27.3	14.8	21	28.5
Zn	53.5	b.d.l.	47.2	62.0	79.0

\* Data from [12]; b.d.l.: below detection limit.

Major element concentrations of the samples from [12] were obtained through a Philips PW2404 X-ray fluorescence spectrometer equipped with a Rh anticathode at the Department of Biological, Geological, and Environmental Sciences at the University of Catania. Trace element concentrations were determined by using a High-Resolution Inductively Coupled Plasma Mass Spectrometer (ThermoFinniganMAT «Element 2», Bremen, Germany), which employs a double-focusing mass analyzer with reverse Nier–Johnson geometry (see [65] for the preparation of samples). Major and trace element concentrations of the samples from [48] were determined via X-ray fluorescence on a Philips PW 1480 spectrometer at Bologna University, Italy, and by using inductively coupled plasma (ICP)-emission and ICP–mass spectrometry at the Center de Recherches Pétrographique et Géochimiques, Service d’Analyses des Roches du CNRS, Vandœuvre, France (see [48] for details).

Overall, as displayed in Figure 7, the major element oxides show quite homogenous distributions between the selected representative samples from both [12] and [48], except for some outliers, as in the case of the higher calcium content in sample gm7 (Table 1, Figure 7a) and lower magnesium and silica contents in sample DF343 from [48] and gm7 (Table 1, Figure 7b,d), respectively.

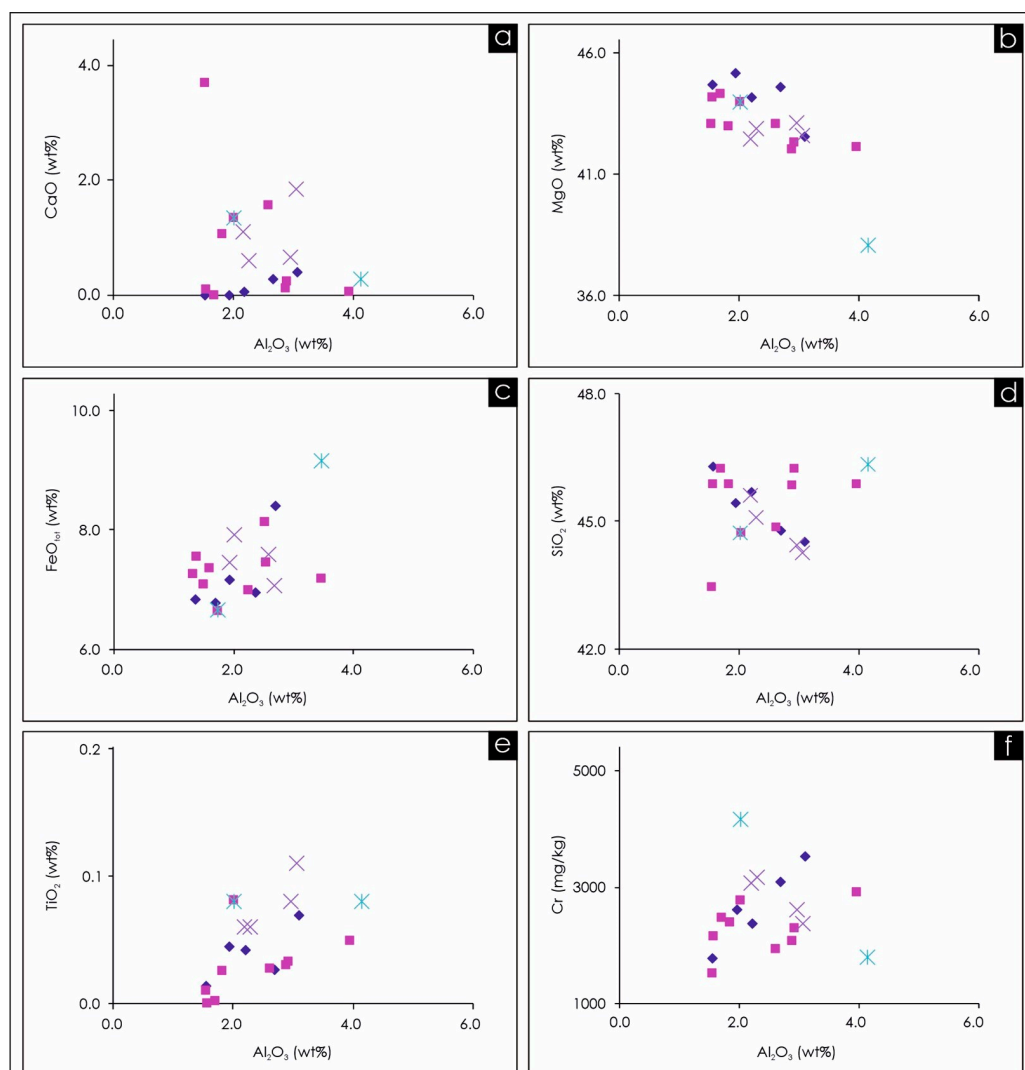


**Figure 7.** Binary diagrams of selected major and minor elements plotted versus  $\text{Al}_2\text{O}_3$  alumina content for the representative selected serpentinites located at the Gimigliano (squares and asterisks) and at Mt. Reventino areas (diamonds and crosses). Data are from [12,48]. From (a–f) please note the various compositional ranges of each element, reflecting the mineralogical variations within the serpentinite rock.

By focusing on the Mt. Reventino quarry, slight differences can be observed in higher contents of calcium, iron, and titanium and lower contents of magnesium and silica in samples from [48] with respect to [12] (Figure 7). In the case of Gimigliano samples, comparisons between the two datasets are limited due to the poorly representative specimens from [48] in this area.

With regard to amounts of trace elements, Cr, Ni, and Co contents are high in all samples. In the Gimigliano specimens, they vary, respectively, from 1525–2905 mg/kg (Table 2), reaching 4157 mg/kg in samples from [48], 1235–2051 mg/kg (Table 2) and 1205–2230 mg/kg in samples from [48], 79.3–110.7 mg/kg (Table 2), and 97–105 in samples from [48]. In the Reventino samples, Cr ranges from 1773 to 3524 mg/kg (Table 3) and 2369 to 3181 mg/kg in samples from [48], Ni ranges from 1829 to 2241 mg/kg (Table 3) and 1486 to 1972 mg/kg in samples from [48], and Co ranges from 71 to 129.7 mg/kg (Table 3) and 71 to 93 in samples from [48] (primordial mantle values: Cr = 3140 mg/kg; Ni = 2110 mg/kg [66]; Co = 105 mg/kg [67]). The Cr number values (Cr# in Table 1), which vary from 13.5 to 23.9 and from 7.6 to 28.0 in samples from [48], are comparable with values

typical of less depleted oceanic peridotites [64], whereas values of the Mg number (Mg#) are quite homogeneous (Mg#: 77.3–81.9) except for the sample DF343 from [48].

The analysis of the Rare Earth Element (REE) patterns normalized to chondrite [68] (Figure 8a) highlights a clear enrichment in the light REEs with respect to the heavy REEs and intermediate REEs, with a La/Yb ratio ranging from 13.8 to 94.3, which is pronounced in the Gimigliano serpentinites. The incompatible elements' patterns normalized to the primordial mantle [69] (Figure 8b) are similar to each other. An enrichment in some elements, with particular regard to Zr (sample gm10) and Hf (samples gm10 and REV4) with respect to the chondrite, is clearly observed, as well as a depletion in Ti (sample gm4).

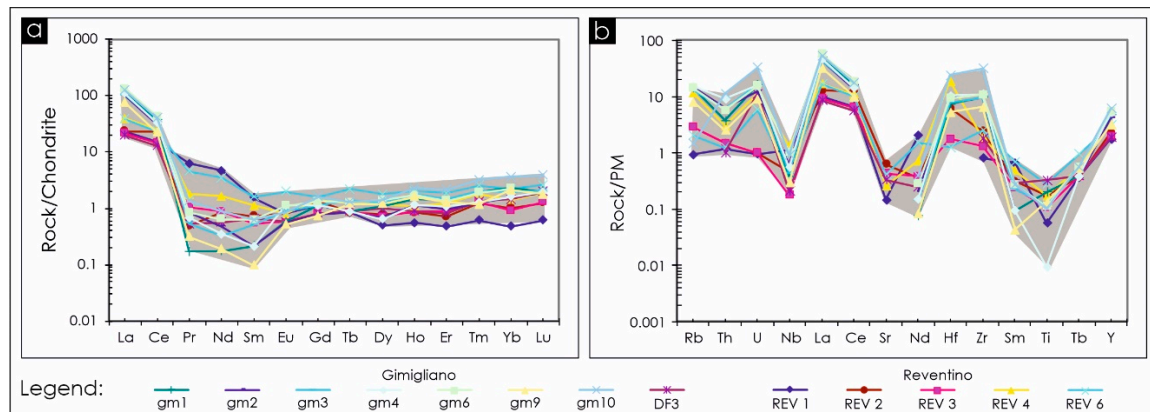


**Figure 8.** Discrimination diagrams normalized to the chondrite (a) and to the primordial mantle (b) for the representative selected serpentinites located at the Gimigliano and Reventino areas. Data are from [12].

These results are comparable, on the whole, with the serpentinites that crop out at the Calabria–Basilicata border (southern Italy) [20], which locally show higher normalized amounts of silica and lower amounts of magnesium with respect to the investigated serpentinites from Sila Piccola (SiO<sub>2</sub>: 43.5–47.3 wt%; MgO: 39.2–44.7 wt%), whereas the mean values of Cr and Ni (Cr: 2560 mg/kg; Ni: 1930 mg/kg) mirror the values observed in the analyzed samples.

Slight differences can be found with the schistose and massive serpentinites quarried in Valmalenco (northern Italy) [70], which show, based on their mean values, higher silica, magnesium, and calcium normalized contents (SiO<sub>2</sub>: 42.7–44.0 wt%; MgO: 42.4–44.0 wt%; CaO: 1.5–2.1 wt%), whereas, also in this case, concentrations of trace elements are in the same ranges (e.g., Ni: 1298–2018 mg/kg; Co: 101–132 mg/kg), with slight LREE enrichments and flat HREE patterns [70].

## 5. Petrophysical Properties

The petrophysical and mechanical behavior of serpentinite rocks from Calabria as stone materials has been reported by [32], where a detailed petrophysical investigation concerning salt crystallization tests, seismic analysis, and compressional strength measurements permitted an understanding of the relationship between compositional and microstructural features and the behavior of such rocks. According to results reported after salt crystallization tests (35 cycles), on the one hand, existing microfractures do open, giving rise to a microfracture network (Figure 9a); on the other hand, salts tend to crystallize within both microfractures and veins, thus triggering the breakage of some specimens on cycles 13–15 (Figure 9b). Moreover, the same authors noticed that, in some cases, the substitution of soluble salts after calcite within microfractures did occur, as well as some forms of decay, such as exfoliation of the surface. Seismic velocity tests carried out on serpentinite, either not involving (NCT) or after (PCT) the salt crystallization test [32], revealed that before the crystallization tests, the average compressional velocity values were in the

range between 6.00 and 7.50 km/s, whereas after the crystallization tests, average values decreased within the range of 5.19–6.78 km/s (Table 4), indicating fracture development inside the rock. This fracturing system has been depicted in detail at the microscale with X-ray microtomography imaging (Figure 9c,d) [33], showing the complex network that develops in serpentinite rocks. The estimation of the Uniaxial Compressive Strength (UCS) ranges from about 76.9 to 191.3 MPa, thus highlighting the mechanical behavior of the serpentinite from Calabria. Moreover, the petrophysical properties of serpentinite from Calabria have been compared with those concerning historical serpentinite quarries located in other localities in the frame of the Mediterranean area in order to compare their behavior (Table 4).

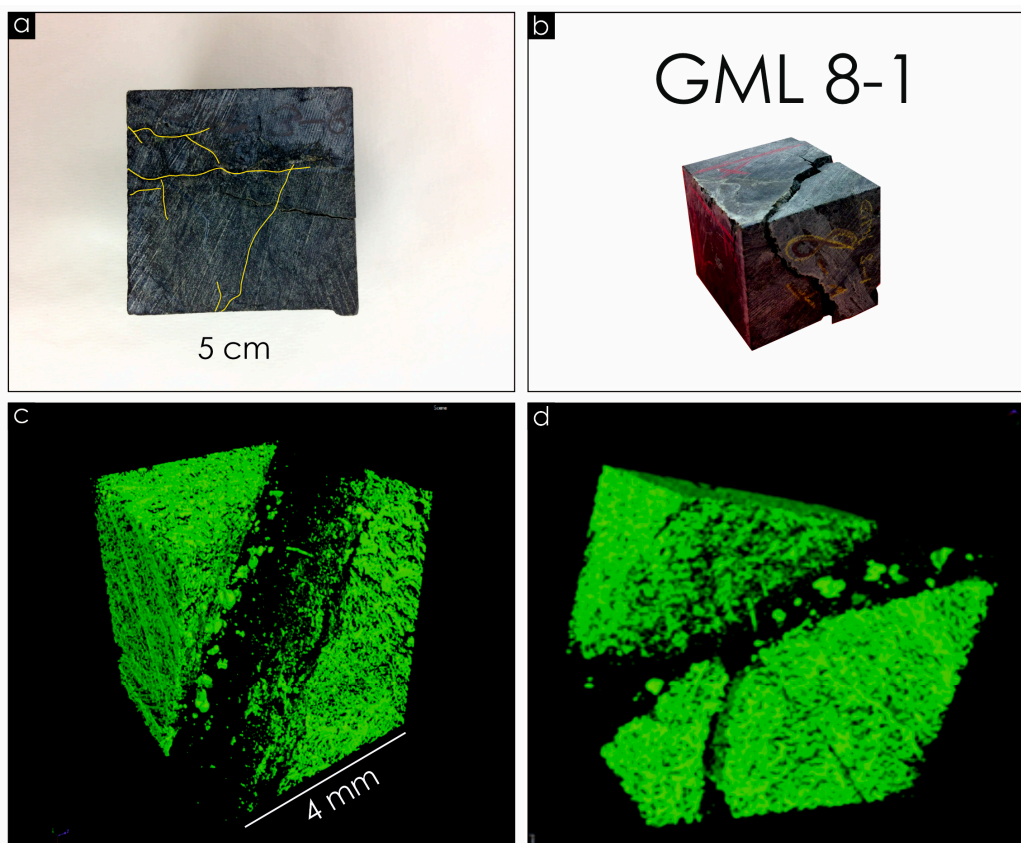


**Figure 9.** Sample cubes selected for the petrophysical investigation: (a) the development of veins (i.e., yellow in the figure) during the salt-crystallization tests; (b) breakage during the tests, controlled by vein development; (c,d) X-ray-computed assisted microtomography imaging showing the 3D arrangement of veins at the microscale.

**Table 4.** Comparisons of Uniaxial Compressive Strength (UCS), rock density ( $\rho$ ), and compressional seismic wave velocity ( $V_p$ ) of different serpentinites reported in the literature.

Source			UCS (MPa)	Parameters $\rho$ (kg/m <sup>3</sup> )	$V_p$ (m/s)
Southern Italy [32]	Northern Calabria (PCT)	m	80.9	2537	5188
		Av	121.7	2604	6155
		M	159.2	2639	6777
		SD	29.7	37	556
	Northern Calabria (NCT)	m	76.9	2578	6027
		Av	140.5	2615	7122
		M	191.3	2633	7918
		SD	47.8	19	518

Table 4. Cont.

Source		UCS (MPa)	Parameters $\rho$ (kg/m <sup>3</sup> )	Vp (m/s)	
Moeche (Spain) [11]	m	24	2600	1859	
	Av	57	2750	4673	
	M	129	2840	5914	
	SD	24	70	1098	
Egypt [9]	m	89	2480	n.a.d.	
	Av	152	2520	n.a.d.	
	M	189	2590	n.a.d.	
	SD	32	30	n.a.d.	
Greece [10]	m	19	2490	4842	
	Av	60	2610	5344	
	M	126	2730	5789	
	SD	27	60	225	
Turkey [71]	m	22	2430	4265	
	Av	54	2564	5018	
	M	77	2660	5461	
	SD	16	58	341	
Southern Spain [72]	Granada	m	331	2658	5532
		Av	346	2662	5646
		M	361	2666	5589
		SD	51	18	457
	Macael (carbonated)	m	139	2704	6024
		Av	227	2796	6078
		M	315	2888	6132
		SD	43	32	309
	Macael (non-carbonated)	m	246	2650	5308
		Av	279	2949	5203
		M	263	2800	5378
		SD	61	134	673

UCS = uniaxial compressional strength;  $\rho$  = rock density; Vp = compressional wave velocity; PCT = post-crystallization test; NCT = non-crystallization test; m = minimum; Av = average; M = maximum; SD = standard deviation; n.a.d. = not available data.

## 6. Discussions and Concluding Remarks

Despite being widely used and marketed as “Green Marble”, peculiar mineralogical, petrographic, geochemical, petrophysical, and petrological features clearly define the serpentinite rocks and make them unique in terms of their use and appearance. Since serpentinite, like all rocks used as building materials, undergo various modifications after their change in service from ophiolite outcrops, where they naturally occur, to building and construction materials, detailed knowledge permits, on the one hand, avoiding and preventing unexpected behavior of serpentinites used as building stones; on the other hand, it provides a useful tool for the univocal identification of serpentinite employed in the monuments, in terms of provenance [12,73,74]. This also holds for the serpentinite of the Sila Piccola Massif (Calabria region, southern Italy), which was exploited over time as a construction material and ornamental stone, as well as for jewelry manufacturing [12,13]. The differences in petrophysical behavior among specimens not affected by crystallization tests (NCT) and after this treatment (PCT) show that NCT specimens are, on average, characterized by higher Vp and UCS values and that the great variability is probably due to the random orientation of microcracks. PCT specimens show a reduction in UCS of about 14% compared to NCT, testifying to their increased weakness, although showing a less porous structure since many fractures have been filled by salts in cycle after cycle. Indeed, historical serpentinite quarries in Sila Piccola Massif, Calabria, show features that encounter, for instance, the American ASTM standards, which require a UCS > 69 MPa,

$\rho > 2.560 \text{ g/cm}^3$ ; therefore, serpentinite from Calabria may be used successfully as a building material and may still constitute an important georesource provided that their detailed characterization must forerun their use in the construction or conservation–restoration of the architectonic heritage.

Comprehensive characterization is also particularly important because it has been reported in the literature that serpentinites from Calabria may contain asbestiform and other fibrous minerals, as shown by the occurrence of chrysotile, tremolite, and actinolite asbestos [13,14,75–77] located within the veins, which could lead to possible health problems due to asbestos fiber exposure (European Directive 2003/18/CE).

In addition, the geochemical signatures of the investigated serpentinites support a potential derivation from native enriched peridotites, as suggested by the Mg# and Cr# values, as well as the low REE enrichments and some of the high-field-strength elements (i.e., Zr and Hf), especially in the Gimigliano serpentinites.

The bulk chemistry shown in Table 1 highlights that Cr and Ni are the most abundant heavy metals detected in the studied serpentinites, and they should be looked after, as a limit value for some toxic elements (e.g., Cr, Ni) in soil and stream water has been established by the Italian government (Legislative Decree N°152 of 3 April 2006), even though, in general, no limit has been established for rocks and minerals. From this perspective, the same thresholds have been considered to assess the potential risk due to the high amounts of heavy metals in the analyzed serpentinites. The contents of both Cr and Ni exceed the maximum admissible amounts for private, public, and residential green use (Limit A, Cr = 150 mg/kg; Ni = 120 mg/kg), as well as commercial and industrial use (Limit B, Cr = 800 mg/kg; Ni = 500 mg/kg). Therefore, the knowledge of geochemical features of serpentinite rocks is another important tool for environmental monitoring, since the weathering of ophiolite outcrops can represent a potential source of toxic elements [26], in particular the first-row transition elements. On the other hand, serpentinites have the ability to sequester carbon dioxide (CO<sub>2</sub>) and provide a highly reactive feedstock for carbonation reactions; indeed, with the use of high-temperature carbonation reactors, alkaline mine wastes, or subsurface reactions involving the injection of CO<sub>2</sub> into serpentinite-hosted aquifers and serpentinitized peridotites, CO<sub>2</sub> can be sequestered in serpentinite that has been mined [78,79].

In conclusion, despite the commercial name (i.e., Green Marble), serpentinite is a peculiar and multifaceted metamorphic rock; therefore, by also considering that, in general, serpentinite lithotypes pose health and environmental issues, a detailed knowledge deriving from a multi-analytical approach (mineralogical, compositional, and petrophysical) is needed when such rocks are employed as either construction materials or for the conservation/restoration of cultural heritage.

**Author Contributions:** Conceptualization, R.P., R.V. and R.C.; methodology, R.P.; investigation, R.P.; resources, R.P. and R.C.; data curation, R.P. and R.V.; writing—original draft preparation, R.P., R.V. and R.C.; writing—review and editing, R.P. and R.V.; visualization, R.V.; supervision, R.C.; project administration, R.C.; funding acquisition, R.P. All authors have read and agreed to the published version of the manuscript.

**Funding:** This research was funded by University of Catania: (a) (PIA<sub>n</sub>o di inCEntivi per la Rlcerca di Ateneo 2020/2022—Pia.Ce.Ri), Grant Number: 22722132153, within the project: “Combined geomatic and petromatic applications: The new frontier of geoscience investigations from field- to micro-scale—(GeoPetroMat)” and (b) PIA<sub>n</sub>o di inCEntivi per la Rlcerca di Ateneo 2020/2022 linea 1 Chance grant number 22722132173 P.I., R. Punturo).

**Data Availability Statement:** Data are from [9–12,32,48,71,72].

**Acknowledgments:** The authors are grateful to M.R. Pinizzotto and to C. Cantara (Sicilian Regional Agency for Environmental Protection, ARPA) for their valuable support in serpentinite sample management and for fruitful discussions on asbestos-related issues. The Syrmep beamline staff at Elettra Synchrotron (Trieste, Italy) is acknowledged for technical support. We thank the three anonymous reviewers for their constructive comments, which helped us to improve the quality and clarity of the manuscript, and Lucas Xiang for the editorial handling of the manuscript.

**Conflicts of Interest:** The authors declare no conflict of interest.

## References

1. Coleman, R.G. Ophiolites: Ancient Oceanic Lithosphere? In *Minerals and Rocks*; Springer: Berlin/Heidelberg, Germany, 1977; Volume 12, ISBN 978-3-642-66675-9.
2. Coleman, R.G.; Jove, C. Geological Origin of Serpentinites. In *The Vegetation of Ultramafic (Serpentine) Soils*; Baker, A.J.M., Proctor, J., Reeves, R.D., Eds.; Intercept Ltd.: Andover, UK, 1993; pp. 1–18.
3. Steinmann, G. Die ophiolitischen Zonen in den mediterranen Kettengebirgen. In *Proceedings of the Comptes Rendus*; Graficas Reunidas: Madrid, Spain, 1927; Volume 2, pp. 637–667.
4. Basley, E.B.; McCallien, W.J. Some Aspects of the Steinmann Trinity, Mainly Chemical. *Q. J. Geol. Soc. Lond.* **1960**, *116*, 365–395. [[CrossRef](#)]
5. Pereira, D.; Peinado, M.; Yenes, M.; Monterrubio, S.; Nespereira, J.; Blanco, J.A. Serpentinites from Cabo Ortegal (Galicia, Spain): A Search for Correct Use as Ornamental Stones. *Geol. Soc. Lond. Spec. Publ.* **2010**, *333*, 81–85. [[CrossRef](#)]
6. Navarro, R.; Pereira, D.; Rodríguez-Navarro, C.; Sebastián-Pardo, E. The Sierra Nevada Serpentinites: The Serpentinites Most Used in Spanish Heritage Buildings. *Geol. Soc. Lond. Spec. Publ.* **2015**, *407*, 101–108. [[CrossRef](#)]
7. Pereira, D.; Blanco, J.A.; Peinado, M. Study on Serpentinites and the Consequence of the Misuse of Natural Stone in Buildings for Construction. *J. Mater. Civ. Eng.* **2013**, *25*, 1563–1567. [[CrossRef](#)]
8. Marinos, P.; Hoek, E.; Marinos, V. Variability of the Engineering Properties of Rock Masses Quantified by the Geological Strength Index: The Case of Ophiolites with Special Emphasis on Tunnelling. *Bull. Eng. Geol. Environ.* **2006**, *65*, 129–142. [[CrossRef](#)]
9. Ismael, I.S.; Hassan, M.S. Characterization of Some Egyptian Serpentinites Used as Ornamental Stones. *Chin. J. Geochem.* **2008**, *27*, 140–149. [[CrossRef](#)]
10. Diamantis, K.; Gartzos, E.; Migiros, G. Study on Uniaxial Compressive Strength, Point Load Strength Index, Dynamic and Physical Properties of Serpentinites from Central Greece: Test Results and Empirical Relations. *Eng. Geol.* **2009**, *108*, 199–207. [[CrossRef](#)]
11. Nespereira, J.; Navarro, R.; Monterrubio, S.; Yenes, M.; Pereira, D. Serpentinite from Moeche (Galicia, North Western Spain). A Stone Used for Centuries in the Construction of the Architectural Heritage of the Region. *Sustainability* **2019**, *11*, 2700. [[CrossRef](#)]
12. Punturo, R.; Fiannacca, P.; Giudice, A.; Pezzino, A.; Cirrincione, R.; Liberi, F.; Piluso, E. Le Cave storiche della “pietra Verde” di Gimigliano e Monte Reventino (Calabria): Studio petrografico e geochimico. *Boll. Della Soc. Gioenia Sci. Nat.* **2004**, *37*, 37–59.
13. Zakrzewska, A.M.; Capone, P.P.; Iannò, A.; Tarzia, V.; Campopiano, A.; Villella, E.; Giardino, R. Calabrian Ophiolites: Dispersion of Airborne Asbestos Fibers during Mining and Milling Operations. *Period. Mineral.* **2008**, *77*, 27–34. [[CrossRef](#)]
14. Punturo, R.; Bloise, A.; Critelli, T.; Catalano, M.; Fazio, E.; Apollaro, C. Environmental Implications Related to Natural Asbestos Occurrences in the Ophiolites of the Gimigliano-Mount Reventino Unit (Calabria, Southern Italy). *Int. J. Environ. Res.* **2015**, *9*, 405–418. [[CrossRef](#)]
15. Piccarreta, G.; Zirpoli, G. Le rocce verdi del Monte Reventino (Calabria). *Boll. Della Soc. Geol. Ital.* **1968**, *88*, 469–488.
16. Ogniben, L. Schema Geologico della Calabria in base ai dati odierni. *Geol. Romana* **1973**, *12*, 243–585.
17. Amodio Morelli, L.; Bonardi, G.; Colonna, V.; Dietrich, D.; Giunta, G.; Ippolito, F.; Liguori, V.; Lorenzoni, S.; Paglionico, A.; Perrone, V.; et al. L’arco calabro-peloritano nell’orogene appenninico-maghrebide. *Mem. Della Soc. Geol. Ital.* **1976**, *17*, 1–60.
18. Spadea, P. Contributo alla conoscenza dei metabasalti ofiolitici della Calabria settentrionale e centrale e dell’Appennino Lucano. *Rendiconti Della Soc. Ital. Mineral. E Petrol.* **1979**, *35*, 251–276.
19. Spadea, P. Calabria-Lucania Ophiolites. *Boll. Di Geofis. Teor. E Appl.* **1994**, *36*, 141–144.
20. Beccaluva, L.; Macciotta, G.; Spadea, P. Petrology and Geodynamic Significance of the Calabria-Lucania Ophiolites. *Rendiconti Della Soc. Ital. Mineral. E Petrol.* **1982**, *38*, 973–987.
21. Morten, L.; Tortorici, L. Geological Framework of the Ophiolite-Bearing Allochthonous Terranes of the Calabrian Arc and Lucanian Apennine. *Accad. Naz. Delle Sci. Detta Dei XL Roma* **1993**, *43*, 145–150.
22. Piluso, E.; Cirrincione, R.; Morten, L. Ophiolites of the Calabrian Peloritan Arc and Their Relationships with the Crystalline Basement (Catena Costiera and Sila Piccola, Calabria, Southern Italy)—GLOM 2000 Excursion Guide-Book. *Ofoliti* **2000**, *25*, 117–140. [[CrossRef](#)]
23. Alvarez, W. Structure of the Monte Reventino Greenschist Folds: A Contribution to Untangling the Tectonic-Transport History of Calabria, a Key Element in Italian Tectonics. *J. Struct. Geol.* **2005**, *27*, 1355–1378. [[CrossRef](#)]
24. Tursi, F.; Bianco, C.; Brogi, A.; Caggianelli, A.; Prosser, G.; Ruggieri, G.; Braschi, E. Cold Subduction Zone in Northern Calabria (Italy) Revealed by Lawsonite–Clinopyroxene Blueschists. *J. Metamorph. Geol.* **2020**, *38*, 451–469. [[CrossRef](#)]

25. Apollaro, C.; Marini, L.; Critelli, T.; Barca, D.; Bloise, A.; De Rosa, R.; Liberi, F.; Miriello, D. Investigation of Rock-to-Water Release and Fate of Major, Minor, and Trace Elements in the Metabasalt–Serpentinite Shallow Aquifer of Mt. Reventino (CZ, Italy) by Reaction Path Modelling. *Appl. Geochem.* **2011**, *26*, 1722–1740. [[CrossRef](#)]
26. Punturo, R.; Ricchiuti, C.; Giorno, E.; Apollaro, C.; Miriello, D.; Visalli, R.; Bloise, A.; Rita, P.M.; Cantaro, C. Potentially Toxic Elements (PTES) in Actinolite and Serpentinite Host Rocks: A Case Study from the Basilicata Region (Italy). *Ofioliti* **2023**, *48*, 93–104. [[CrossRef](#)]
27. Campopiano, A.; Olori, A.; Zakrzewska, A.M.; Capone, P.P.; Iannò, A. Chemical-Mineralogical Characterisation of Greenstone from San Mango d’Aquino. *Prev. Today* **2009**, *5*, 25–38.
28. Bloise, A.; Catalano, M.; Barrese, E.; Gualtieri, A.F.; Bursi Gandolfi, N.; Capella, S.; Belluso, E. TG/DSC Study of the Thermal Behaviour of Hazardous Mineral Fibres. *J. Therm. Anal. Calorim.* **2016**, *123*, 2225–2239. [[CrossRef](#)]
29. Cirrincione, R.; Fazio, E.; Fiannacca, P.; Ortolano, G.; Pezzino, A.; Punturo, R. The Calabria–Peloritani Orogen, a Composite Terrane in Central Mediterranean; Its Overall Architecture and Geodynamic Significance for a Pre-Alpine Scenario around the Tethyan Basin. *Period. Mineral.* **2015**, *84*, 701–749. [[CrossRef](#)]
30. Festa, V.; Langone, A.; Caggianelli, A.; Rottura, A. Dike Magmatism in the Sila Grande (Calabria, Southern Italy): Evidence of Pennsylvanian–Early Permian Exhumation. *Geosphere* **2010**, *6*, 549–566. [[CrossRef](#)]
31. Ortolano, G.; Visalli, R.; Fazio, E.; Fiannacca, P.; Godard, G.; Pezzino, A.; Punturo, R.; Sacco, V.; Cirrincione, R. Tectono-Metamorphic Evolution of the Calabria Continental Lower Crust: The Case of the Sila Piccola Massif. *Int. J. Earth Sci.* **2020**, *109*, 1295–1319. [[CrossRef](#)]
32. Punturo, R.; Ricchiuti, C.; Mengel, K.; Apollaro, C.; Rosa, R.D.; Bloise, A. Serpentinite-Derived Soils in Southern Italy: Potential for Hazardous Exposure. *J. Mediterr. Earth Sci.* **2018**, *10*, 51–61. [[CrossRef](#)]
33. Bloise, A.; Ricchiuti, C.; Lanzafame, G.; Punturo, R. X-Ray Synchrotron Microtomography: A New Technique for Characterizing Chrysotile Asbestos. *Sci. Total Environ.* **2020**, *703*, 135675. [[CrossRef](#)]
34. Pugnaloni, A.; Giantomassi, F.; Lucarini, G.; Capella, S.; Bloise, A.; Di Primio, R.; Belluso, E. Cytotoxicity Induced by Exposure to Natural and Synthetic Tremolite Asbestos: An in Vitro Pilot Study. *Acta Histochem.* **2013**, *115*, 100–112. [[CrossRef](#)] [[PubMed](#)]
35. Cavallo, A.; Rimoldi, B. Chrysotile Asbestos in Serpentinite Quarries: A Case Study in Valmalenco, Central Alps, Northern Italy. *Environ. Sci. Process. Impacts* **2013**, *15*, 1341–1350. [[CrossRef](#)] [[PubMed](#)]
36. Langer, A.M. Identification and Enumeration of Asbestos Fibers in the Mining Environment: Mission and Modification to the Federal Asbestos Standard. *Regul. Toxicol. Pharmacol. RTP* **2008**, *52*, S207–S217. [[CrossRef](#)]
37. Gamble, J.F.; Gibbs, G.W. An Evaluation of the Risks of Lung Cancer and Mesothelioma from Exposure to Amphibole Cleavage Fragments. *Regul. Toxicol. Pharmacol. RTP* **2008**, *52*, S154–S186. [[CrossRef](#)] [[PubMed](#)]
38. Suzuki, Y.; Yuen, S.R.; Ashley, R. Short, Thin Asbestos Fibers Contribute to the Development of Human Malignant Mesothelioma: Pathological Evidence. *Int. J. Hyg. Environ. Health* **2005**, *208*, 201–210. [[CrossRef](#)] [[PubMed](#)]
39. Ortolano, G.; Fazio, E.; Visalli, R.; Alsop, G.I.; Pagano, M.; Cirrincione, R. Quantitative Microstructural Analysis of Mylonites Formed during Alpine Tectonics in the Western Mediterranean Realm. *J. Struct. Geol.* **2020**, *131*, 103956. [[CrossRef](#)]
40. Ortolano, G.; Pagano, M.; Visalli, R.; Angi, G.; D’Agostino, A.; Muto, F.; Tripodi, V.; Critelli, S.; Cirrincione, R. Geology and Structure of the Serre Massif Upper Crust: A Look in to the Late-Variscan Strike–Slip Kinematics of the Southern European Variscan Chain. *J. Maps* **2022**, *18*, 314–330. [[CrossRef](#)]
41. Cirrincione, R.; Ortolano, G.; Pezzino, A.; Punturo, R. Poly-Orogenic Multi-Stage Metamorphic Evolution Inferred via P–T Pseudosections: An Example from Aspromonte Massif Basement Rocks (Southern Calabria, Italy). *Lithos* **2008**, *103*, 466–502. [[CrossRef](#)]
42. Pezzino, A.; Angi, G.; Fazio, E.; Fiannacca, P.; Lo Giudice, A.; Ortolano, G.; Punturo, R.; Cirrincione, R.; De Vuono, E. Alpine Metamorphism in the Aspromonte Massif: Implications for a New Framework for the Southern Sector of the Calabria–Peloritani Orogen, Italy. *Int. Geol. Rev.* **2008**, *50*, 423–441. [[CrossRef](#)]
43. Fazio, E.; Ortolano, G.; Visalli, R.; Alsop, I.; Cirrincione, R.; Pezzino, A. Strain Localization and Sheath Fold Development during Progressive Deformation in a Ductile Shear Zone: A Case Study of Macro-to Micro-Scale Structures from the Aspromonte Massif, Calabria. *Ital. J. Geosci.* **2018**, *137*, 208–218. [[CrossRef](#)]
44. Ortolano, G.; Visalli, R.; Cirrincione, R.; Rebay, G. PT-Path Reconstruction via Unraveling of Peculiar Zoning Pattern in Atoll Shaped Garnets via Image Assisted Analysis: An Example from the Santa Lucia Del Mela Garnet Micaschists (Northeastern Sicily-Italy). *Period. Mineral.* **2014**, *83*, 257–297. [[CrossRef](#)]
45. Ietto, A.; Barillaro, A.M. L’Unità di San Donato quale margine deformato cretaco-paleogenico del bacino di Lagonegro (Appennino meridionale-Arco Calabro). *Boll. Della Soc. Geol. Ital.* **1993**, *111*, 193–215.
46. Ietto, F.; Ietto, A. Sviluppo e Annegamento Di Un Sistema Carbonatico Piattaforma Bacino Nel Trias Superiore Della Catena Costiera Calabrese. *Boll. Della Soc. Geol. Ital.* **1998**, *117*, 313–331.
47. Perrone, V. Une nouvelle hypothese sur la position paleogeographique et l’evolution tectonique des Unites de Verbicaro et de San Donato (region Calabro-Lucanienne; Italie): Implication sur le limite Alpes-Appennines en Calabre. *Comptes Rendus Acad. Sci. Paris* **1996**, *322*, 877–884.
48. Liberi, F.; Morten, L.; Piluso, E. Geodynamic Significance of Ophiolites within the Calabrian Arc. *Isl. Arc* **2006**, *15*, 26–43. [[CrossRef](#)]

49. de Roever, E.W.F. Lawsonite-Albite-Facies Metamorphism near Fuscaldo, Calabria (Southern Italy): Its Geological Significance and Petrological Aspects. *GUA Pap. Geol. Amst.* **1972**, *3*, 1–172.
50. Guerrera, F.; Martin-Algarra, A.; Perrone, V. Late Oligocene-Miocene Syn-/Late-Orogenic Successions in Western and Central Mediterranean Chains from the Betic Cordillera to the Southern Apennines. *Terra Nova* **1993**, *5*, 525–544. [[CrossRef](#)]
51. Cello, G.; Invernizzi, C.; Mazzoli, S. Structural Signature of Tectonic Processes in the Calabrian Arc, Southern Italy: Evidence from the Oceanic-Derived Diamante-Terranova Unit. *Tectonics* **1996**, *15*, 187–200. [[CrossRef](#)]
52. Tortorici, L.; Catalano, S.; Monaco, C. Ophiolite-Bearing Mélanges in Southern Italy. *Geol. J.* **2009**, *44*, 153–166. [[CrossRef](#)]
53. Alvarez, W. A Former Continuation of the Alps. *GSA Bull.* **1976**, *87*, 891–896. [[CrossRef](#)]
54. Dietrich, D. Sense of Overthrust Shear in the Alpine Nappes of Calabria (Southern Italy). *J. Struct. Geol.* **1988**, *10*, 373–381. [[CrossRef](#)]
55. Cello, G.; Morten, L.; De Francesco, A.M. The Tectonic Significance of the Diamante-Terranova Unit (Calabria, Southern Italy) in the Alpine Evolution of the Northern Sector of the Calabrian Arc. *Boll. Della Soc. Geol. Ital.* **1991**, *110*, 685–694.
56. Graessner, T.; Schenk, V.; Bröcker, M.; Mezger, K. Geochronological Constraints on the Timing of Granitoid Magmatism, Metamorphism and Post-Metamorphic Cooling in the Hercynian Crustal Cross-Section of Calabria. *J. Metamorph. Geol.* **2000**, *18*, 409–421. [[CrossRef](#)]
57. Thomson, S.N. Fission Track Analysis of the Crystalline Basement Rocks of the Calabrian Arc, Southern Italy: Evidence of Oligo-Miocene Late-Orogenic Extension and Erosion. *Tectonophysics* **1994**, *238*, 331–352. [[CrossRef](#)]
58. Zecchin, M.; Caffau, M.; Di Stefano, A.; Maniscalco, R.; Lenaz, D.; Civile, D.; Muto, F.; Critelli, S. The Messinian Succession of the Crotone Basin (Southern Italy) II: Facies Architecture and Stratal Surfaces across the Miocene-Pliocene Boundary. *Mar. Pet. Geol.* **2013**, *48*, 474–492. [[CrossRef](#)]
59. Lanzafame, G.; Zuffa, G.G. Geologia e Petrografia del Foglio Bisignano (Bacino del Crati, Calabria). *Geol. Romana* **1976**, *15*, 223–270.
60. Spadea, P.; Tortorici, L.; Lanzafame, G. Serie ofiolitifere nell'area compresa fra Tarsia e Spezzano Albanese (Calabria): Stratigrafia, petrografia, rapport strutturali. *Mem. Della Soc. Geol. Ital.* **1976**, *17*, 135–174.
61. Lanzafame, G.; Spadea, P.; Tortorici, L. Mesozoic Ophiolites of Northern Calabria and Lucanian Apennines (Southern Italy). *Ofioliti* **1979**, *4*, 173–182.
62. Dubois, R. La Suture Calabro-Apenninique Cretace-Eocene et L'ouverture Tyrrhénienne Neogene; Étude Pétrographique et Structurale de la Calabre Centrale. Ph.D. Thesis, Université Paris VI, Paris, France, 1976.
63. Bloise, A.; Punturo, R.; Catalano, M.; Miriello, D.; Cirrincione, R. Naturally Occurring Asbestos (NOA) in Rock and Soil and Relation with Human Activities: The Monitoring Example of Selected Sites in Calabria (Southern Italy). *Ital. J. Geosci.* **2016**, *135*, 268–279. [[CrossRef](#)]
64. Bonatti, E.; Michael, P.J. Mantle Peridotites from Continental Rifts to Ocean Basins to Subduction Zones. *Earth Planet. Sci. Lett.* **1989**, *91*, 297–311. [[CrossRef](#)]
65. Punturo, R.; Censi, P.; Lo Giudice, A. Trace Element Measurements on Selected Reference Materials Using HR-ICP-MS after Microwave Digestion: An Application to Archaeometric Studies. *Period. Mineral.* **2003**, *72*, 103–121.
66. Sun, S.; McDonough, W.F. Chemical and Isotopic Systematics of Oceanic Basalts: Implications for Mantle Composition and Processes. *Geol. Soc. Lond. Spec. Publ.* **1989**, *42*, 313–345. [[CrossRef](#)]
67. Jagoutz, E.; Palme, H.; Baddenhausen, H.; Blum, K.; Cendales, M.; Dreibus, G.; Spettel, B.; Lorenz, V.; Wänke, H. The Abundances of Major, Minor and Trace Elements in the Earth's Mantle as Derived from Primitive Ultramafic Nodules. In *Lunar and Planetary Science Conference, 10th, Houston, TX, USA, 19–23 March 1979, Proceedings*; Pergamon Press, Inc.: Houston, TX, USA, 1979; Volume 2, pp. 2031–2050.
68. Boynton, W.V. Geochemistry of the Rare Earth Elements: Meteorite Studies. In *Rare Earth Element Geochemistry*; Enderson, P., Ed.; Elsevier: Amsterdam, The Netherlands, 1989; pp. 63–114.
69. McDonough, W.F. Constraints on the Composition of the Continental Lithospheric Mantle. *Earth Planet. Sci. Lett.* **1990**, *101*, 1–18. [[CrossRef](#)]
70. Cavallo, A. "Serpentino Della Valmalenco" (Central Alps, Northern Italy): A Green Dimension Stone with Outstanding Properties. *Resour. Policy* **2022**, *75*, 102467. [[CrossRef](#)]
71. Kurtulus, C.; Bozkurt, A.; Endes, H. Physical and Mechanical Properties of Serpentinized Ultrabasic Rocks in NW Turkey. *Pure Appl. Geophys.* **2012**, *169*, 1205–1215. [[CrossRef](#)]
72. Navarro, R.; Pereira, D.; Gimeno, A.; Del Barrio, S. Influence of Natural Carbonation Process in Serpentinites Used as Construction and Building Materials. *Constr. Build. Mater.* **2018**, *170*, 537–546. [[CrossRef](#)]
73. Pereira, M.D.; Peinado, M.; Blanco, J.A.; Yenes, M. Geochemical Characterization of Serpentinites at Cabo Ortegal, Northwestern Spain. *Can. Mineral.* **2008**, *46*, 317–327. [[CrossRef](#)]
74. Pereira, D. A Report on Serpentinites in the Context of Heritage Stone Resources. *Episodes J. Int. Geosci.* **2012**, *35*, 478–480. [[CrossRef](#)]
75. Bloise, A.; Barca, D.; Gualtieri, A.F.; Pollastri, S.; Belluso, E. Trace Elements in Hazardous Mineral Fibres. *Environ. Pollut.* **2016**, *216*, 314–323. [[CrossRef](#)]

76. Bloise, A.; Belluso, E.; Critelli, T.; Catalano, M.; Apollaro, C.; Miriello, D.; Barrese, E. Amphibole Asbestos and Other Fibrous Minerals in the Meta-Basalt of the Gimigliano-Mount Reventino Unit (Calabria, South-Italy). *Rend. Online Della Soc. Geol. Ital.* **2012**, *21*, 847–848.
77. Bloise, A.; Miriello, D.; De Rosa, R.; Vespasiano, G.; Fuoco, I.; De Luca, R.; Barrese, E.; Apollaro, C. Mineralogical and Geochemical Characterization of Asbestiform Todorokite, Birnessite, and Ranciéite, and Their Host Mn-Rich Deposits from Serra D’Aiello (Southern Italy). *Fibers* **2020**, *8*, 9. [[CrossRef](#)]
78. Dichicco, M.C.; Laurita, S.; Paternoster, M.; Rizzo, G.; Sinisi, R.; Mongelli, G. Serpentinite Carbonation for CO<sub>2</sub> Sequestration in the Southern Apennines: Preliminary Study. *Energy Procedia* **2015**, *76*, 477–486. [[CrossRef](#)]
79. Power, I.M.; Wilson, S.A.; Dipple, G.M. Serpentinite Carbonation for CO<sub>2</sub> Sequestration. *Elements* **2013**, *9*, 115–121. [[CrossRef](#)]

**Disclaimer/Publisher’s Note:** The statements, opinions and data contained in all publications are solely those of the individual author(s) and contributor(s) and not of MDPI and/or the editor(s). MDPI and/or the editor(s) disclaim responsibility for any injury to people or property resulting from any ideas, methods, instructions or products referred to in the content.